Journal of Magnetism and Magnetic Materials xxx (2008) 0–0

Contents lists available at ScienceDirect

Journal of Magnetism and Magnetic Materials

journal homepage: www.elsevier.com/locate/agee

Structural and magnetic characterization of $LaSrMnO_3$ thin films deposited by laser ablation on MgO substrates

I.T. Gomes[a], B.G. Almeida[a,*], A.M.L. Lopes[b], J.P. Araújo[b], J. Barbosa[a], J.A. Mendes[a,c]

[a]*Departamento de Física, Universidade do Minho, Campus de Gualtar, 4710-057 Braga, Portugal*

[b]*Departamento de Física and IFIMUP, Univ. Porto, R. Campo Alegre 687, 4169-007 Porto, Portugl*

[c]*ESEIG, Instituto Politécnico Porto, Rua D. Sancho I, 981, 4480-876 Vila do Conde, Portugal*

A R T I C L E I N F O

Elsevier use only
Article history:
Received date here
Received in revised form date here
Accepted date here
Available online date here

Keywords: Type keywords here, separated;

A B S T R A C T

$La_{2/3}Sr_{1/3}MnO_{3-\delta}$ thin films were deposited by laser ablation on MgO substrates under low oxygen pressure cool down. Their structural and magnetic properties are presented. The magnetic and electrical resistivity measurements indicate a reduction of the Curie and the metal-insulator transition temperatures due to the formation of magnetic inhomogeneneous films, where clusters of a metallic phase are mixed in a magnetically disordered insulating matrix. By a low angle X-ray reflectivity study we show that the thin films are chemically inhomogeneous with an oxygen deficiency in bulk of the film when compare with the film/air interfacial region.

1. Introduction

In recent years, the rare-earth manganites exhibiting colossal magnetoresistance have been attracting much scientific and technological interest [1-3]. In the perovskite-type $La_{1-x}A_xMnO_3$ (A = divalent alkaline-earth ions) system, a ferromagnetic coupling between the Mn ions develops in the concentration range x = 0.2-0.6, due to the double exchange mechanism [2]. Above the Curie temperature (T_C), in the paramagnetic state, charge transport is thermally activated and the electrical resistivity is high. Near T_C, the electrical resistivity has a maximum and then drops to a metallic-like character below a characteristic metal-insulator transition temperature T_{MI} ($T_{MI} \sim T_C$). In the temperature region near T_C, the application of a magnetic field strongly decreases the electrical resistivity and this deeply negative magnetoresistance is called colossal magnetoresistance (CMR). For the particular case of lanthanum strontium manganate ($La_{1-x}Sr_xMnO_3$: LSMO) the Curie temperature can attain relatively high values, reaching 380 K for x = 1/3. Combined with its CMR characteristics, this then makes it a promising material for room-temperature magnetic sensors, recording devices or bottom electrode in the fabrication of ferroelectric memories [1,2].

In thin film form, it is known that stress or oxygen deficiencies generate magnetic inhomogeneities [3,4]. Then, the presence of less magnetically ordered insulating clusters, along with the ferromagnetic metallic phase, induce a suppression of ferromagnetic order and metallic conductivity. In order to deepen this problem, here, under-oxidized thin films of LSMO were deposited by laser ablation and their structural and magnetic properties were characterized.

2. Experimental details

The LSMO thin films were prepared by pulsed laser ablation on (001)MgO substrates. The depositions were done with a KrF excimer laser (wavelength λ = 248 nm), at a fluence of 2 J/cm^2 and 10 Hz repetition rate. The pulse duration was 25 ns and the target-to-substrate distance was 5 cm. Prior to deposition, the substrates were cleaned in an ultra-sound bath with ethanol. They were then put in the ablation chamber that was evacuated to a base pressure of 5×10^{-5} mbar. The oxygen pressure during preparation was 0.3 mbar and the substrate temperature was 700 ºC. After the deposition, the oxygen pressure was maintained at 2 mbar while the films were slowly cooled to room temperature. With this cooling procedure, the films became slightly under-oxidized in its preparation.

For the laser ablation targets, polycrystalline samples of $La_{2/3}Sr_{1/3}MnO_3$ were prepared by the gel combustion method. Stoichiometric amounts of La_2O_3, $SrCO_3$, and $MnCO_3$ were used as starting materials. These oxides/carbonates were converted into metal nitrates by adding nitric acid and dissolved in distilled water to obtain a clear solution. Citric acid (CA) and urea were used as fuel/complexing agents with a molar ratio of [urea]/[salts] = 3 and [CA]/[salts] = 2. By adding ammonia the pH of solution was adjusted to 6.5. Subsequently, the solution was heated with stirring to evaporate most of the solvent water. The resultant gel precursor was then decomposed at about 250 °C and a black precursor powder was obtained. In order to get the desired laser ablation targets this powder was ground and pelletized and then annealed at temperatures from 500 ºC to 1400 °C.

The structural studies were performed by X-ray diffraction (XRD) and were carried out with a Siemens D5000 diffractometer using Cu Kα radiation. The magnetic properties were measured with a Quantum Design MPMS SQUID magnetometer. The electrical resistivity measurements were performed in the temperature range 15 – 300 K, with the standard four probe in-line technique.

The X-ray diffraction spectra measured on the laser ablation targets showed that they were polycrystalline and composed by $La_{0.67}Sr_{0.33}MnO_3$ with a rhombohedrically distorted perovskite structure (R3c system). The

* Corresponding author. Tel.: +351253604063; fax: +351253678981.
E-mail address: bernardo@fisica.uminho.pt.

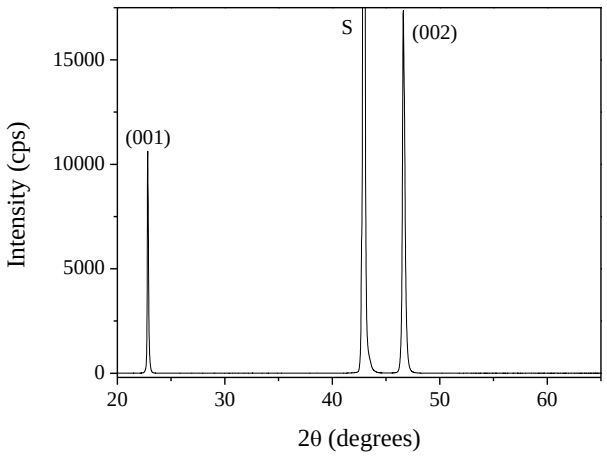

Figure 1: X-ray diffraction spectrum obtained on a $La_{0.67}Sr_{0.33}MnO_3$ thin film deposited on (001)MgO. The peak marked with an S is from the substrate

corresponding value of the pseudo-cubic lattice parameter was a = 0.388 nm, slightly higher than the reference value ($a_{ref.}$ = 0.3873 nm [2]). The lattice parameters of the films were determined referring to the pseudo –cubic structure.

3. Results and discussion

Figure 1 shows the X-ray diffraction spectrum obtained on a LSMO thin film deposited on (001)MgO. The results show that the films were composed by lanthanum strontium manganate with a perovskite type structure. They were oriented, presenting a (001) preferred growth direction. The peaks were fitted using pseudo-Voigt functions in order to determine their angular positions and integral widths. The grain size obtained from the fitted (001) X-ray diffraction peak width, using the Scherrer equation [5], was 122 nm. The lattice parameter determined from the (001) fitted peak position was a_{film} = 0.3881 nm, slightly higher than the one for bulk LSMO with the same composition (a_{bulk} = 0.3873 nm). This indicates a distortion of the films lattice, where the mismatch between the LSMO films and the MgO substrate induces an in-plane compression and an out-of-plane expansion of the unit cell parameters, consistent with the known results for LSMO films on MgO.

The temperature dependence of the magnetization was measured in the temperature range from 5 K to 380 K. The curves were obtained by initially cooling the sample under an applied magnetic field of H = 50 Oe (field cooled, FC) and then measuring its magnetization with increasing temperature (applied field of H = 50Oe). Subsequently, after reaching 380 K, the sample was re-cooled, this time with no applied magnetic field (zero-field-cooled, ZFC) and the magnetization measurements were again performed with increasing temperature, under the same magnetic field of H = 50 Oe. Figure 2 shows the magnetization obtained on a $La_{0.67}Sr_{0.33}MnO_3$ thin film, under this field-cooling and zero-field-cooling conditions. The obtained Curie temperature for this sample is T_C ~ 280 K. The ZFC magnetization curve is below the FC one and has a maximum at T ~ 50 K presents. This maximum is associated with irreversibility due to magnetically disordered clusters [1].

Figure 3 shows the temperature dependence of the electrical resistivity, normalized by its value at T = 300 K. The curve presents a maximum characteristic of a metal-to-insulator-like transition, at T_{MI} = 177 K. The electrical resistivity severely drops below T_{MI} but never fully reaches the metallic behavior, starting to rise again below ~47 K. This behavior, along with the smaller Curie temperature as compared to the bulk LSMO with the same composition ($T_{C,bulk}$ = 380 K), is due to the presence of magnetic inhomogeneities, where clusters of the metallic phase are mixed in a magnetically disordered insulating matrix, hindering the formation of the fully metallic phase. In addition this is supported by the broad peak of the resistivity curve which correlates well with the broad transition observed in the magnetization data. This further suggests that a distribution of ferromagnetic metallic critical temperatures occurs. The considerably lower value of T_{MI} than T_C suggests that the ferromagnetism sets in gradually and that ferromagnetic metallic state is only attained at T_{MI} when this phase percolates over the insulator one.

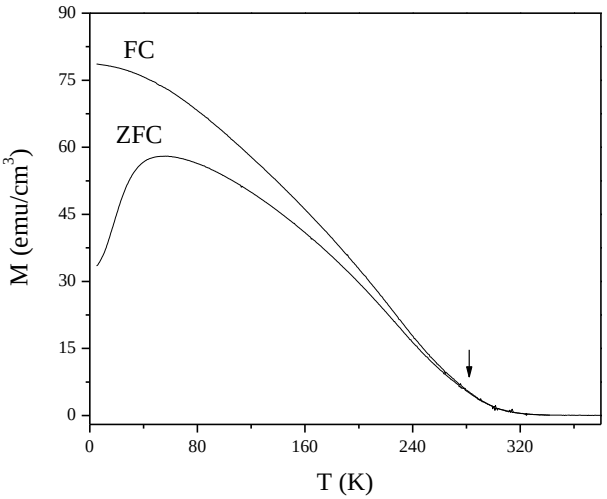

Figure 2: Temperature dependence of the magnetization, measured on a LSMO thin film deposited on MgO. The curves were obtained under zero-field-cooled (ZFC) and field cooled conditions (FC, H = 50 Oe)

To further characterize the structure, measurements of the low angle X-ray specular reflectivity were performed on the films. Figure 4a) shows the reflectivity of a $La_{0.67}Sr_{0.33}MnO_3$ film measured in the 2θ range 0.4º-4º. Since the refraction index of matter is below that of air, when the X-ray beam impinges the surface with sufficiently low incident angle it doesn't penetrate the film and is totally reflected. Then, up to the critical angle of total reflection (θ_C) the spectrum presents a plateau on the reflectivity curve (fig. 4a). In fact, the refraction index at X-ray wavelength can be written as [6,7]:

$$n = 1 - \frac{\lambda^2 r_e \rho_e}{2\pi} + i\beta \qquad (1)$$

where β is due to absorption, λ is the X-ray wavelength ($\lambda_{CuK\alpha 1}$ = 0.154056 nm), r_e is the classical electron radius and ρ_e is the electronic density of the material. Above the critical angle the X-ray beam penetrates the film, giving a reflectivity curve that strongly decreases with increasing incident angle due to the Fresnel reflectivity.

On figure 4a), two large well separated bumps, marked with vertical arrows, are superimposed on the on the spectrum, indicating the presence of a thin top layer film with different electronic density than the LSMO film [6]. Additionally, the spectrum shows the presence of small oscillations, as observed on the enlargement of the reflectivity curve presented in the inset of figure 4a). They are called Kiessig fringes [6,8,9] and are due to the interference between the waves reflected at the air/film and film/substrate interfaces, thus corresponding to the film-thickness oscillations. The total thickness of the film is then obtained from the Kiessig fringes through [9]:

$$m = -\frac{1}{2} + \frac{2D}{\lambda}\sqrt{\cos^2(\theta_C) - \cos^2(\theta_m)} \qquad (1)$$

where m is the order of the fringes, θ_m the angle of the maximum of the m^{th}

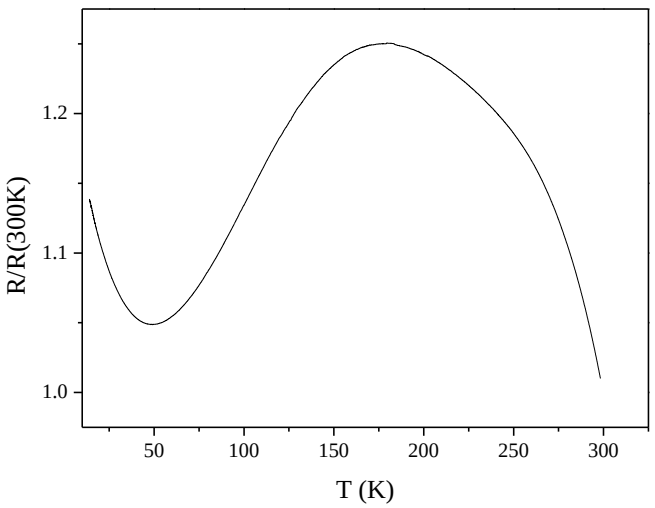

Figure 3: Temperature dependence of the electrical resistivity, normalized by its value at 300 K, measured on the temperature range 15 – 300 K.

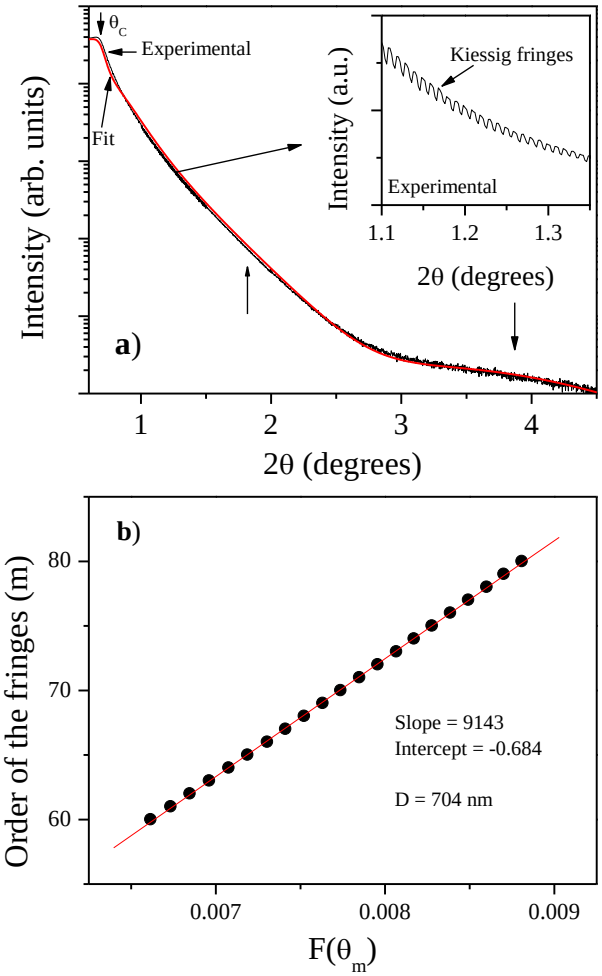

Figure 4: Low angle X-ray specular reflectivity spectrum a) obtained on a $La_{0.67}Sr_{0.33}MnO_3$ thin film deposited on MgO. The inset shows an enlargement of the curve in the 2θ region 1.1 - 1.35º. In b) is the order of the Kiessig fringes for different $F(\theta_m) = \sqrt{\cos^2(\theta_C) - \cos^2(\theta_m)}$ values.

fringe and D is the film's thickness. This equation is essentially the Bragg equation for the fringes, taking into account the refraction of the X-ray beam. Equation (1) then leads to a linear relation between the order of the fringes and the function $F(\theta) = \sqrt{\cos^2(\theta_C) - \cos^2(\theta)}$, as shown in figure 4b). From the slope of the straight line a film's thickness of 704 nm is obtained.

In order to fit the reflectivity curves a simple trilayer model was used, including the MgO substrate, the LSMO film and the top layer. Assuming perfect interfaces, without any roughness, the reflectivity (R) of this trilayer structure can be calculated by [6]:

$$R = \left| \frac{r_{0,1} + r_{1,2} e^{-iq_1 d_1} + r_{2,S} e^{-i(q_1 d_1 + q_2 d_2)} + r_{0,1} r_{1,2} r_{2,S} e^{-2iq_2 d_2}}{1 + r_{0,1} r_{1,2} e^{-2iq_1 d_1} + r_{1,2} r_{2,S} e^{-2iq_2 d_2} + r_{2,S} r_{0,1} e^{-2i(q_1 d_1 + q_2 d_2)}} \right|^2 \quad (2)$$

where $q_i = \frac{4\pi}{\lambda}\sqrt{n^2 - \cos^2(\theta)}$ is the scattering vector on layer i (with refraction index n_i and incident angle θ), $r_{i,j} = (q_i - q_j)/(q_i + q_j)$ is the reflection coefficient at the interface between layers i and j and d_i is the thickness of layer i. In equation (2) the sub-indexes refer to: 0 - air, 1 - top layer, 2 - LSMO layer and S to the MgO substrate. To account for the roughness at the interfaces, each of the reflectivities $r_{i,j}$ were multiplied by the factor $e^{-q_i q_j \sigma_j^2}$ [6], where σ_j is the root mean square height on the interface between layer i and j. To reduce the number of fitting parameters, the refraction index of the substrate and of air (q_{air} = 1), and the total thickness of the trilayer structure, determined from the Kiessig fringes (fig. 4b), were kept fixed. Also, the roughness of the LSMO and the top layers were considered equal (overall roughness of the film) and the roughness of the substrate was fixed at σ_S = 5 Å. The remaining parameters, namely, the refraction indexes of the LSMO layer and the top layer, the film's roughness and the thickness of the top layer, were allowed to vary. From the fitted refraction indexes, the electronic densities ρ_e can be determined through equation (1). The reflectivity spectra of the thin films were then fitted using a Levenberg-Marquardt algorithm that iteratively varied the parameters until the weighted mean square difference between the experimental and calculated reflectivity of the system was minimized.

The fitted values obtained for the top layer thickness and the film's roughness were 2.1 nm and 9.5 nm, respectively. The obtained electronic densities ρ_e were 2.7×10^{24} cm^{-3} for the LSMO layer and 1.7×10^{24} cm^{-3}, for the top layer. The electronic densities are related to the number of electrons per "particle" (N_e) and density (ρ) of the material, through $\rho_e = N_e \rho N_A/M_0$, where N_A is the Avogadro's number and M_0 is the molar mass. For $La_{0.67}Sr_{0.33}MnO_3$, N_e = 100, M_0 = 223.5 g/mol and ρ = 6.0 g/cm³ [10], for a bulk ceramic, so that $\rho_{e,b} \sim 1.62\times10^{24}$ cm^{-3}. Comparing with the bulk, in the film the obtained electronic density of the LSMO layer is higher, due to the relative excess of La, Sr and Mn (with more electrons), as compared to oxygen, originated by the under-oxidation of the films. On the other hand, due to the oxidation on exposure to the air, the top layer is formed with a proportion of oxygen to lanthanum, strontium and manganese more near from $La_{0.67}Sr_{0.33}MnO_3$. This is then accompanied by a corresponding decrease of the electronic density towards the bulk value, as observed from the fitted results obtained for the top layer.

4. Conclusions

Lanthanum stronthium manganese under-oxidized thin films were deposited by laser ablation on MgO substrates and their structural and magnetic properties were characterized. The magnetic and electrical resistivity measurements indicated a reduction of the Curie and the metal-insulator transition temperatures due to the formation of magnetic inhomogeneneous films, where clusters of a metallic phase are mixed in a magnetically disordered insulating matrix. The magnetic inhomogeneity was likely caused by the low oxygen pressure during the cooling process from deposition temperature to room temperature, yielding oxygen deficient thin films with a wide distribution of ferromagnetic/metallic critical temperatures. This oxygen inhomogeneity was confirmed by the low angle X-ray reflectivity study presented.

References

[1] K. Dorr, J. Phys. D: Appl. Phys., 39, R125 (2006)
[2] A-M Haghiri-Gosnet, J-P Renard, J. Phys. D: Appl. Phys., 36, R127 (2003)
[3] P. Murugavel, P. Padhan, W. Prellier, J. Phys.: Condens. Matter, 18, 3377 (2006)
[4] K. H. Ahn, T. Lookman, A. R. Bishop, Nature 428 401 (2004)
[5] B.D. Cullity, "Elements of X-Ray Diffraction", Addison-Wesley, Reading MA, (1978)
[6] A. Gibaud, Chapter 3 of "X-ray and neutron reflectivity: principles and applications", Editors: J. Daillant, A. Gibaud, Springer, Heidelberg, (1999)
[7] J Daillant, M Alba, Rep. Prog. Phys., 63, 1725 (2000)
[8] H. Kiessig, Ann. Phys. Leipzig, 402, 769 (1931)
[9] B. Harbecke, B. Heinz, V. Offermann, W. Theiss, In: G. Bauer, W. Richter (Eds.), "Optical characterization of epitaxial semiconductor layers", Springer-Verlag, Berlin (1996)
[10] Y.F. Chen, L. Sun, Y. Pan, Y. Tao, Z.G. Liu, N.B. Ming, Mat. Lett., 27, 139 (1996)